



Semnan University

# Mechanics of Advanced Composite Structures

journal homepage: <http://macs.journals.semnan.ac.ir>

## Precision Closed-form Solution for Out-of-plane Vibration of Rectangular Plates via Trigonometric Shear Deformation Theory

K. Khorshidi\*, M. Khodadadi

Department of Mechanical Engineering, Faculty of Engineering, Arak University, Arak, Iran

### PAPER INFO

#### Paper history:

Received 2015-12-26

Revision Received 2016-02-09

Accepted 2016-02-23

#### Keywords:

Vibration

Precision closed-form solution

Trigonometric shear deformation theory

### ABSTRACT

In this study, the new refine trigonometric shear deformation plate theory is used to study the out-of-plane vibration of the rectangular isotropic plates with different boundary conditions. The novelty of the research is that the analytical precision closed-form solution is developed without any use of approximation for a combination of six different boundary conditions; specifically, two opposite edges are simply supported hard and any of the other two edges can be simply supported hard, clamped or free. The equations of motion and natural boundary conditions, using Hamilton's principle are derived. The present analytical precision closed-form solution can be obtained with any required accuracy and can be used as benchmark. Based on a comparison with the previously published results, the accuracy of the results is shown. Finally, the effect of boundary conditions, variations of aspect ratios and thickness ratios on natural frequency parameters is shown and the relation between natural frequencies for different plates is examined and discussed in detail.

© 2016 Published by Semnan University Press. All rights reserved.

## 1. Introduction

Moderately thick plates are important structural elements. They are widely used in various engineering applications such as aircrafts, space structures, ships and submarines. In order to solve plate problems, two main steps must be taken: the choice of the plate theory and the type of solution method. The most commonly used plate theories can be classified into four main categories: Classical Thin Plate Theory (CPT) (based on the hypothesis that straight lines normal to the undeformed midplane remain straight and normal to the deformed mid plane and do not undergo thickness stretching.), Leissa [1], First-order Shear Deformation Plate Theory (FSDT) (based on the assumption that straight lines normal to the undeformed midplane remain straight but not necessarily normal to the deformed midplane and in this theory the transverse shear strain distribution is assumed to be constant through the plate thickness and therefore shear correction factor is required to account for the strain energy of shear deformation), Reissner [2,3], Mindlin[4], and Kim

and Cho [5], Third-order Shear Deformation Plate Theory (TSDT) and three-dimensional elasticity theory (3-D). According to a comprehensive survey of literature, it is found that a wide range of researches has been carried out on free vibration of the rectangular and circular plates that most of them have used CPT, FSDT, TSDT and 3-D [6]. In order to deal with moderately thick plates, the trigonometric shear deformation plate theory was introduced to take into account the transverse shear strains and rotary inertia. Five variables are used in this theory to describe the deformation: three displacements of the middle surface and two rotations. In case of flat plates (without geometric imperfections), the in-plane displacements are uncoupled from the transverse displacement and rotations. Several publications can be found, in existing literature, concerning the investigation of trigonometric shear deformation plate theory. Ferreira et al. [7] analyzed symmetric composite plates using a meshless method based on global multi quadric radial basis functions. They used the trigonometric shear

\*Corresponding author, Tel.: +98-863-2625050; Fax: +98-863-4173450

E-mail address: k-khorshidi@araku.ac.ir

deformation theory which this trigonometric theory uses trigonometric functions through the thickness direction, allowing for zero transverse shear stresses at the top and bottom surfaces of the plate. Xiang and Wang [8] considered the free vibration analysis of symmetric laminated composite plates using the trigonometric shear deformation theory. Mantari et al. [9, 10] developed a new trigonometric shear deformation theory for isotropic and composite laminated and sandwich plates. Tounsi et al. [11] presented a Refined Trigonometric Shear Deformation Theory (RTSDT) by taking into account the transverse shear deformation effects for the thermo-elastic bending analysis of the functionally graded sandwich plates. Tornabene et al. [12] developed a general formulation of a 2D higher-order equivalent single layer theory including the stretching and zig-zag effects for free vibrations of thin and thick doubly-curved laminated composite shells and panels with different curvatures. Rango et al [13] presented the formulation of an enriched macro element suitable for analyzing the free vibration response of the composite plate based on the Trigonometric Shear Deformation Theory (TSDT). Sahoo and Singh [14] proposed a new trigonometric zig-zag theory for the static analysis of the laminated composite and the sandwich plates. When the equations of motion are derived using each of plate theories, these partial differential equations must be solved through numerical methods, semi-analytical methods or exact analytical methods. The exact free vibration and buckling analysis of rectangular plates has been studied by many researchers using CPT, FSDT and TSDT. Vel and Batra [15] presented a three-dimensional exact solution for free and forced vibrations of simply supported functionally graded rectangular plates. HosseiniHashemi and Arsanjani [16] derived the dimensionless equations of motion from the Mindlin plate theory to study the transverse vibration of thick rectangular plates without further usage of any approximate method. Hosseini-Hashemi et al [17] presented an exact solution to study the buckling of in-plane loaded isotropic rectangular plates with different boundary conditions. The proposed rectangular plates have two opposite edges simply-supported, while all possible combinations of free, simply-supported and clamped boundary conditions are applied to the other two edges. Hosseini-Hashemi et al [18] investigated the structural-acoustic radiation of vibrating rectangular Mindlin plates in different combinations of classical boundary conditions. Hosseini-Hashemi et al [19] presented an analytical solution for free vibration analysis of moderately thick rectangular plates, which is composed of Functionally Graded Materials (FGMs) and is supported by either Winkler or Pasternak elastic foundations. Khorshidi [20-21] ana-

lyzed the dynamic response of the moderately thick isotropic rectangular plates using an exact closed-form procedure. Hosseini-Hashemi et al. [22] presented an exact closed-form procedure for free vibration analysis of moderately thick rectangular plates having two opposite edges simply supported (i.e. Levy-type rectangular plates) based on the Reissner-Mindlin plate theory. Liu and Xing [23] obtained an exact closed-form solution for free vibrations of orthotropic rectangular Mindlin plates using the separation of variables. Dozio [24] presented an exact solution for free vibration of rectangular cross-ply laminated plates with at least one pair of opposite edges simply supported using refined kinematic theories of variable order. Leissa [25] presented an exact solution for the six cases of vibrating thin rectangular plates having two opposite sides simply-supported and the Ritz method for the remaining 15 cases which involved the possible combinations of clamped, simply-supported, and free edge conditions. Liew et al. [26] analyzed the transverse vibration of thick rectangular plates using the Rayleigh-Ritz procedure. Liew et al. [27] present the vibration analysis of shear deformable plates, which is formulated on the basis of first-order Mindlin theory. Malik and Bert [28] presented an accurate three-dimensional elasticity solution for free vibrations of six types of plates having free lateral surfaces, two opposite sides simply supported, and two other sides having combinations of simply supported, clamped, and free boundary conditions via the differential quadrature method. Liew et al. [29] formulated three-dimensional Ritz method for the vibration analysis of homogeneous, thick, rectangular plates with arbitrary combinations of boundary constraints. Zhou et al. [30] presented three-dimensional vibration analysis of thick rectangular plates using Chebyshev polynomial and Ritz method.

The objective of this study is to determine the free vibration response of rectangular plates using the trigonometric shear deformation plate theory. Such equations for moderately thick plates are not available in the literature. In order to fill this apparent void, the present work is carried out by providing the exact free vibration analysis for six cases of a rectangular plate having two opposite sides simply supported. The other two edges may be given by any possible combination of free, simply-supported and clamped boundary conditions. The integrated equations of motion in terms of the resultant stresses are derived from the trigonometric shear deformation plate theory for moderately thick rectangular plates. This is done by considering the transverse shear deformation and rotary inertia. The exact transverse deflection and the exact displacements along  $x_1$  and  $x_2$  axes are derived for the

first time. The present analytical solution can be obtained with any required accuracy and can be used as benchmark. Based on a comparison with the previously published results, the accuracy of the results is shown. Finally, the effect of boundary conditions, variations of aspect ratios and thickness ratios on natural frequency parameters and the relation between natural frequencies for different plates are examined and discussed in detail.

## 2. Governing Equations of Motion

A flat, isotropic, rectangular plate with uniform thickness  $h$ , length  $a$ , width  $b$ , modulus of elasticity  $E$ , Poisson's ratio  $\nu$ , and density  $\rho$  is shown in Fig. 1. The displacement components  $u$  and  $v$  are the in-plane displacements of middle surface in  $x_1$  and  $x_2$  directions respectively and  $w$  is the deflection of middle surface in  $x_3$  direction. The two edges of the plate parallel to the  $x_2$  direction are assumed to be simply supported while the other two edges may have any combinations of clamped, free or simply supported boundary conditions.

Based on the trigonometric shear deformation theory, the displacement field can be described as the following [10]:

$$u(x_1, x_2, x_3, t) = -x_3 \frac{\partial w(x_1, x_2, t)}{\partial x_1} + f(x_3)\varphi_1(x_1, x_2, t) \quad (1a)$$

$$v(x_1, x_2, x_3, t) = -x_3 \frac{\partial w(x_1, x_2, t)}{\partial x_2} + f(x_3)\varphi_2(x_1, x_2, t) \quad (1b)$$

$$w(x_1, x_2, x_3, t) = w(x_1, x_2, t), \quad (1c)$$

Where  $\varphi_1$  and  $\varphi_2$  are the rotations of the transverse normal about  $x_1$  and  $x_2$  axes, respectively and

$$f(x_3) = \frac{h}{\pi} \sin\left(\frac{\pi x_3}{h}\right). \quad (2)$$

In Eqs. (1a) and (1b) the sinusoidal function is assigned according to the shear stress distribution through the thickness of the plate. Using Hamilton's principle (see appendix A), the governing differential equations of motion are as follows:

$$\begin{aligned} \frac{\partial^2 M_1}{\partial x_1^2} + 2 \frac{\partial^2 M_{12}}{\partial x_1 \partial x_2} + \frac{\partial^2 M_2}{\partial x_2^2} \\ = I_1 \frac{\partial^2 w}{\partial t^2} \\ - I_2 \left( \frac{\partial^4 w}{\partial t^2 \partial x_1^2} + \frac{\partial^4 w}{\partial t^2 \partial x_2^2} \right) \\ + I_3 \left( \frac{\partial^3 \varphi_1}{\partial x_1 \partial t^2} + \frac{\partial^3 \varphi_2}{\partial x_2 \partial t^2} \right) \end{aligned} \quad (3a)$$

$$\frac{\partial N_{s1}}{\partial x_1} + \frac{\partial N_{s21}}{\partial x_2} - N_{Tc1} = -I_3 \frac{\partial^3 w}{\partial t^2 \partial x_1} + I_4 \frac{\partial^2 \varphi_1}{\partial t^2} \quad (3b)$$

$$\frac{\partial N_{s2}}{\partial x_2} + \frac{\partial N_{s21}}{\partial x_1} - N_{Tc2} = -I_3 \frac{\partial^3 w}{\partial t^2 \partial x_2} + I_4 \frac{\partial^2 \varphi_2}{\partial t^2} \quad (3c)$$

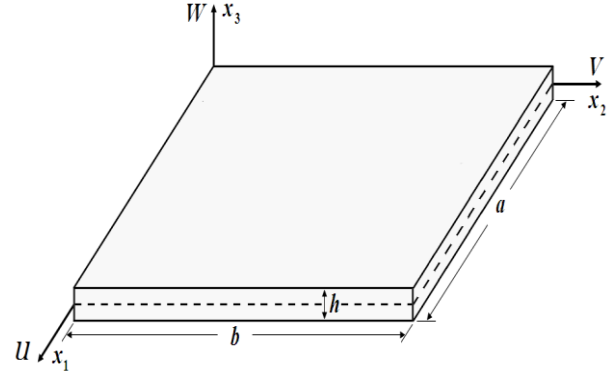


Figure 1. The geometry of a rectangular plate

Where the stress resultants ( $M_{ij}$ ,  $M_i$ ,  $N_{sij}$ ,  $N_{si}$  and  $N_{Tci}$ ) are exhibited in appendix A.

The governing differential equations of motion in terms of displacement field ( $w$ ,  $\varphi_1$  and  $\varphi_2$ ) can be rewritten as what follows:

$$\begin{aligned} B_1 \left( \frac{\partial^4 w}{\partial x_1^4} + 2 \frac{\partial^4 w}{\partial x_2^2 \partial x_1^2} + \frac{\partial^4 w}{\partial x_2^4} \right) \\ - B_2 \left( \frac{\partial^3 \varphi_1}{\partial x_1^3} + \frac{\partial^3 \varphi_1}{\partial x_2^2 \partial x_1} \right. \\ \left. + \frac{\partial^3 \varphi_2}{\partial x_2^3} + \frac{\partial^3 \varphi_2}{\partial x_2 \partial x_1^2} \right) + I_1 \frac{\partial^2 w}{\partial t^2} \end{aligned} \quad (4a)$$

$$\begin{aligned} - I_2 \left( \frac{\partial^4 w}{\partial t^2 \partial x_1^2} + \frac{\partial^4 w}{\partial t^2 \partial x_2^2} \right) \\ + I_3 \left( \frac{\partial^3 \varphi_1}{\partial t^2 \partial x_1} + \frac{\partial^3 \varphi_2}{\partial t^2 \partial x_2} \right) = 0 \\ B_2 \left( \frac{\partial^3 w}{\partial x_1^3} + \frac{\partial^4 w}{\partial x_2^2 \partial x_1} \right) - B_3 \left( \frac{\partial^2 \varphi_1}{\partial x_1^2} + B_5 \frac{\partial^2 \varphi_1}{\partial x_2^2} \right) \\ + B_4 \varphi_1 - B_3 B_6 \frac{\partial^2 \varphi_2}{\partial x_2 \partial x_1} \end{aligned} \quad (4b)$$

$$\begin{aligned} - I_3 \frac{\partial^4 w}{\partial t^2 \partial x_1} + I_4 \frac{\partial^2 \varphi_2}{\partial t^2} = 0 \\ B_2 \left( \frac{\partial^3 w}{\partial x_2^3} + \frac{\partial^4 w}{\partial x_1^2 \partial x_2} \right) - B_3 \left( \frac{\partial^2 \varphi_2}{\partial x_2^2} + B_5 \frac{\partial^2 \varphi_2}{\partial x_1^2} \right) \\ + B_4 \varphi_2 - B_3 \frac{\partial^2 \varphi_1}{\partial x_2 \partial x_1} \end{aligned} \quad (4c)$$

$$- I_3 \frac{\partial^4 w}{\partial t^2 \partial x_2} + I_4 \frac{\partial^2 \varphi_1}{\partial t^2} = 0$$

Where

$$B_1 = \frac{Eh^3}{(1-\nu^2)}, \quad (5a)$$

$$B_2 = \frac{EA_0}{(1-\nu^2)}, \quad (5b)$$

$$B_3 = \frac{EB_0}{(1-\nu^2)}, \quad (5c)$$

$$B_4 = \frac{EC_0}{(1-\nu^2)}, \quad (5d)$$

$$A_0 = \int_{-\frac{h}{2}}^{\frac{h}{2}} x_3 f(x_3) dx_3, \quad (5e)$$

$$B_0 = \int_{-\frac{h}{2}}^{\frac{h}{2}} [f(x_3)]^2 dx_3, \quad (5f)$$

$$C_0 = \int_{-\frac{h}{2}}^{\frac{h}{2}} \left[ \frac{\partial f(x_3)}{\partial x_3} \right]^2 dx_3. \quad (5f)$$

$$B_5 = \frac{1-\nu}{2} \quad (5g)$$

$$B_6 = \frac{1+\nu}{2} \quad (5h)$$

For generality and convenience, the coordinates are normalized with respect to the plate planar dimensions and the following nondimensional terms are introduced.

$$X_1 = \frac{x_1}{a}, X_2 = \frac{x_2}{b}, \eta = \frac{b}{a}, \tau = \frac{h}{a}, \quad (6a-6g)$$

$$\tilde{w} = \frac{w}{a}, \tilde{\varphi}_1 = \varphi_1, \quad (6a-6g)$$

$$\tilde{\varphi}_2 = \varphi_2, \quad (6a-6g)$$

$$\beta = a\omega^2 \sqrt{\frac{\rho h}{D}}, \quad D = \frac{Eh^3}{12(1-\nu^2)}. \quad (7a,7b)$$

Where  $\omega$  is the vibration frequency of the plate,  $\beta$  is the frequency parameter,  $D$  is the flexural rigidity,  $\eta$  is aspect ratio,  $\tau$  is thickness ratio and

$$\tilde{\varphi}_1(X_1, X_2, t) = \varphi_1(x_1, x_2) e^{i\omega t}, \quad \tilde{\varphi}_2(X_1, X_2, t) = \varphi_2(x_1, x_2) e^{i\omega t}, \quad (8a)$$

$$\tilde{w}(X_1, X_2, t) = \frac{w(x_1, x_2)}{a} e^{i\omega t}. \quad (8b)$$

Substituting nondimensional terms into Eq. (4), the nondimensional governing differential equations of motion are expressed as follows:

$$\nabla^4 \tilde{w} + \left( \frac{\beta^2 \tau^2}{12} \right) \nabla^2 \tilde{w} - \beta^2 \tilde{w} - (12a_0) \nabla^2 (\tilde{\varphi}_{1,1} + \tilde{\varphi}_{2,2}) - (a_0 \beta^2 \tau^2) (\tilde{\varphi}_{1,1} + \tilde{\varphi}_{2,2}) = 0, \quad (9a)$$

$$\nabla^2 \tilde{w}_{,1} + \left( \frac{\beta^2 \tau^2}{12} \right) \tilde{w}_{,1} - \left( \frac{b_0 B_6}{a_0} \right) \nabla^2 \tilde{\varphi}_1 - \left( \frac{b_0 B_5}{a_0} \right) (\tilde{\varphi}_{1,1} + \tilde{\varphi}_{2,2})_{,1} + \left( \frac{c_0 B_6}{\tau^2 a_0} - \frac{\beta^2 \tau^2}{12} \right) \tilde{\varphi}_1 = 0, \quad (9b)$$

$$\nabla^2 \tilde{w}_{,2} + \left( \frac{\beta^2 \tau^2}{12} \right) \tilde{w}_{,2} - \left( \frac{b_0 B_6}{a_0} \right) \nabla^2 \tilde{\varphi}_2 - \left( \frac{b_0 B_5}{a_0} \right) (\tilde{\varphi}_{1,1} + \tilde{\varphi}_{2,2})_{,2} + \left( \frac{c_0 B_6}{\tau^2 a_0} - \frac{\beta^2 \tau^2}{12} \right) \tilde{\varphi}_2 = 0. \quad (9c)$$

Where comma-subscript convention represents the partial differentiation with respect to the normalized coordinates and

$$a_0 = \frac{A_0}{h^3}, \quad b_0 = \frac{B_0}{h^3}, \quad c_0 = \frac{C_0}{h^3}. \quad (10a-10c)$$

According to trigonometric shear deformation plate theory, the boundary conditions for an edge parallel to the  $x_1$  ( $x_2 = 0$  or  $x_2 = b$ ) are given by:

$$\text{Hard simply support boundary conditions:} \\ \tilde{w} = 0, \quad \tilde{\varphi}_1 = 0, \quad M_2 = 0, \quad N_{s2} = 0. \quad (11a)$$

$$\text{Clamped boundary conditions:} \\ \tilde{w} = 0, \quad \tilde{\varphi}_1 = 0, \quad \tilde{\varphi}_2 = 0, \quad \tilde{w}_{,2} = 0. \quad (11b)$$

$$\text{Free boundary conditions:} \\ V_1 = 0, \quad N_{s12} = 0, \quad M_2 = 0, \quad N_{s2} = 0. \quad (11c)$$

Where

$$V_1 = \frac{\partial M_1}{\partial x_1} + 2 \frac{\partial M_{21}}{\partial x_2} \quad (11d)$$

Corresponding boundary conditions for the simply supported edge at both  $x_1 = 0$  or  $x_1 = a$  are obtained by interchanging subscripts 1 and 2 in equations (11).

After differentiating Eqs. (9b) and (9c) with respect to  $x_1$  and  $x_2$ , respectively, the two obtained equations should be added together. Thus, we have the following equations:

$$\nabla^4 \tilde{w} + \left( \frac{\beta^2 \tau^2}{12} \right) \nabla^2 \tilde{w} = \left( \frac{b_0}{a_0} \right) \nabla^2 (\tilde{\varphi}_{1,1} + \tilde{\varphi}_{2,2}) - \left( \frac{B_5 c_0}{\tau^2 a_0} - \frac{b_0 \beta^2 \tau^2}{12 a_0} \right) (\tilde{\varphi}_{1,1} + \tilde{\varphi}_{2,2}), \quad (12)$$

And the Eq. (9a) can be rewritten as follows:

$$\nabla^4 \tilde{w} + \left( \frac{\beta^2 \tau^2}{12} \right) \nabla^2 \tilde{w} - \beta^2 \tilde{w} = (12a_0) \nabla^2 (\tilde{\varphi}_{1,1} + \tilde{\varphi}_{2,2}) + (2a_0 \beta^2 \tau^2) (\tilde{\varphi}_{1,1} + \tilde{\varphi}_{2,2}) \quad (13)$$

In order to solve Eqs. (9a)–(9c), it is necessary to obtain  $\tilde{w}$ , first. Next, substituting Eq. (12) into Eq. (13), the potential function  $\tilde{\varphi}_{1,1} + \tilde{\varphi}_{2,2}$  can be given by the following equation

$$(\tilde{\varphi}_{1,1} + \tilde{\varphi}_{2,2}) = e_1 \nabla^4 \tilde{w} + e_2 \nabla^2 \tilde{w} + e_3 \tilde{w}, \quad (14a)$$

Where

$$e_1 = \frac{(12a_0^2 - b_0) \tau^2}{6a_0 c_0 (v - 1)}, \quad (14b)$$

$$e_2 = \frac{(12a_0^2 - b_0) \beta^2 \tau^4}{72a_0 c_0 (v - 1)}, \quad (14c)$$

$$e_3 = -\frac{b_0 \beta^2 \tau^2}{6a_0 c_0 (1 - v)}. \quad (14d)$$

Considering Eqs. (12-14a) and after some mathematical manipulations, the following equation can be obtained:

$$\nabla^6 \tilde{w} + a_1 \nabla^4 \tilde{w} + a_2 \nabla^2 \tilde{w} + a_3 \tilde{w} = 0 \quad (15)$$

Where

$$a_1 = \frac{-3c_0(-1+v) + (12a_0^2 - b_0)\beta^2\tau^4}{6(12a_0^2 - b_0)\tau^2} \quad (16a)$$

$$a_2 = \frac{\beta^2(b_0(144 - \beta^2\tau^4) + 6(c_0 - c_0v + a_0^2\beta^2\tau^4))}{144(12a_0^2 - b_0)} \quad (16b)$$

$$a_3 = \frac{\beta^2(6c_0(-1+v) + b_0\beta^2\tau^4)}{12(12a_0^2 - b_0)\tau^2}. \quad (16c)$$

Eq. (15) can be written as what follows:

$$(\nabla^2 - p_1)(\nabla^2 - p_2)(\nabla^2 - p_3)\tilde{w} = 0, \quad (17)$$

Where  $p_1$ ,  $p_2$  and  $p_3$  are the roots of following equation:

$$z^3 + a_1z^2 + a_2z + a_3 = 0. \quad (18)$$

Based on the superposition principle we can write the following solution to Eq. (15), as:

$$\tilde{w} = W_1 + W_2 + W_3. \quad (19)$$

Where  $W_1$ ,  $W_2$  and  $W_3$  are potentials satisfying the differential equations:

$$(\nabla^2 - p_1)\tilde{w} = W_1, \quad (20a)$$

$$(\nabla^2 - p_2)\tilde{w} = W_2, \quad (20b)$$

$$(\nabla^2 - p_3)\tilde{w} = W_3, \quad (20c)$$

And the potential functions  $W_1$ ,  $W_2$  and  $W_3$  are defined as follows:

$$\nabla^2 W_1 + \alpha_1^2 W_1 = 0, \quad (21a)$$

$$\nabla^2 W_2 + \alpha_2^2 W_2 = 0, \quad (21b)$$

$$\nabla^2 W_3 + \alpha_3^2 W_3 = 0, \quad (21c)$$

Where

$$\alpha_1^2 = -p_1 = \frac{-1}{6U} \left( 2^{\frac{4}{3}}(a_1^2 - 3a_2) - 2a_1U + 2^{\frac{2}{3}}U^2 \right), \quad (22a)$$

$$\alpha_2^2 = -p_2 = \frac{-1}{12U} \left( 2i2^{\frac{1}{3}}(i + \sqrt{3})(a_1^2 - 3a_2) - 4a_1U - 2^{\frac{2}{3}}(i + \sqrt{3})U^2 \right), \quad (22b)$$

$$\alpha_3^2 = -p_3 = \frac{-1}{12U} \left( -2i2^{\frac{1}{3}}(-i + \sqrt{3})(a_1^2 - 3a_2) - 4a_1U + 2^{\frac{2}{3}}(i + \sqrt{3})U^2 \right), \quad (22c)$$

$$U = \left( -2a_1^3 + 9a_1a_2 - 27a_3 + \sqrt{-4(a_1^2 - 3a_2)^3 + (2a_1^3 - 9a_1a_2 + 27a_3)^2} \right)^{\frac{1}{3}}. \quad (22d)$$

Substituting Eqs. (14a) and (19) into Eq. (9), the nondimensional rotations can be expressed as the following:

$$\tilde{\varphi}_1 = C_1W_{1,1} + C_2W_{2,1} + C_3W_{3,1} + C_4g_1(X_1, X_2, t), \quad (23a)$$

$$\tilde{\varphi}_2 = C_5W_{1,2} + C_6W_{2,2} + C_7W_{3,2} + C_8g_2(X_1, X_2, t). \quad (23b)$$

In order to find the coefficient  $C_i$  ( $i = 1, 2, 3, 4, 5, 6, 7, 8$ ), the following coefficients are obtained by substituting Eqs. (23a) and (23b) into Eqs. (9),:

$$C_{i(i=1,2,3)} = \frac{C_{i+4}}{\tau^2(-12\alpha_i^2 + \beta^2\tau^2)} \quad (24a)$$

$$C_4 = C_8 = 1. \quad (24b)$$

and

$$\nabla^2 g_1 + \alpha_4^2 g_1 = 0, \quad (25a)$$

$$\nabla^2 g_2 + \alpha_4^2 g_2 = 0. \quad (25b)$$

Where

$$\alpha_4^2 = -\frac{6c_0(-1+v) + b_0\beta^2\tau^4}{6b_0(-1+v)\tau^2}. \quad (26)$$

Substituting Eq. (23) into Eq. (9a), the following equation is obtained as:

$$g_{1,1} + g_{2,2} = 0. \quad (27)$$

The potential functions  $W_4$  so that simultaneously satisfies Eqs. (25) and (27), and it is defined as follows:

$$\nabla^2 W_4 + \alpha_4^2 W_4 = 0. \quad (28)$$

Finally, the  $\tilde{\varphi}_1$ ,  $\tilde{\varphi}_2$  and  $\tilde{w}$  are introduced as what follows:

$$\tilde{w} = W_1 + W_2 + W_3, \quad (29a)$$

$$\tilde{\varphi}_1 = C_1W_{1,1} + C_2W_{2,1} + C_3W_{3,1} + W_{4,2}, \quad (29b)$$

$$\tilde{\varphi}_2 = C_1W_{1,2} + C_2W_{2,2} + C_3W_{3,2} + W_{4,1}, \quad (29c)$$

and

$$\nabla^2 W_1 + \alpha_1^2 W_1 = 0, \quad (30a)$$

$$\nabla^2 W_2 + \alpha_2^2 W_2 = 0, \quad (30b)$$

$$\nabla^2 W_3 + \alpha_3^2 W_3 = 0, \quad (30c)$$

$$\nabla^2 W_4 + \alpha_4^2 W_4 = 0. \quad (30d)$$

Using the separation of variables method, one set of solutions for Eq. (30) can be written as what follows:

$$W_1 = [A_1 \sinh(\mu_1 X_2) + A_2 \cosh(\mu_1 X_2)] \sin(\theta_1 X_1) + [A_3 \sinh(\mu_1 X_2) + A_4 \cosh(\mu_1 X_2)] \cos(\theta_1 X_1), \quad (31a)$$

$$W_2 = [A_5 \sinh(\mu_2 X_2) + A_6 \cosh(\mu_2 X_2)] \sin(\theta_2 X_1) + [A_7 \sinh(\mu_2 X_2) + A_8 \cosh(\mu_2 X_2)] \cos(\theta_2 X_1), \quad (31b)$$

$$W_3 = [A_9 \sin(\mu_3 X_2) + A_{10} \cos(\mu_3 X_2)] \sin(\theta_3 X_1) + [A_{11} \sin(\mu_3 X_2) + A_{12} \cos(\mu_3 X_2)] \cos(\theta_3 X_1), \quad (31c)$$

$$W_4 = [A_{13} \sinh(\mu_4 X_2) + A_{14} \cosh(\mu_4 X_2)] \sin(\theta_4 X_1) + [A_{15} \sinh(\mu_4 X_2) + A_{16} \cosh(\mu_4 X_2)] \cos(\theta_4 X_1). \quad (31d)$$

$$W_4 = [A_{13} \sinh(\mu_4 X_2) + A_{14} \cosh(\mu_4 X_2)] \sin(\theta_4 X_1) + [A_{15} \sinh(\mu_4 X_2) + A_{16} \cosh(\mu_4 X_2)] \cos(\theta_4 X_1). \quad (31d)$$

$$W_4 = [A_{13} \sinh(\mu_4 X_2) + A_{14} \cosh(\mu_4 X_2)] \sin(\theta_4 X_1) + [A_{15} \sinh(\mu_4 X_2) + A_{16} \cosh(\mu_4 X_2)] \cos(\theta_4 X_1). \quad (31d)$$

Where

$$\alpha_1^2 = \mu_1^2 - \theta_1^2, \quad \theta_1^2 > 0, \quad \mu_1^2 > 0, \quad (32a)$$

$$\alpha_2^2 = \mu_2^2 - \theta_2^2, \quad \theta_2^2 > 0, \quad \mu_2^2 > 0, \quad (32b)$$

$$\alpha_3^2 = \mu_3^2 + \theta_3^2, \quad \theta_3^2 > 0, \quad \mu_3^2 > 0, \quad (32c)$$

$$\alpha_4^2 = \mu_4^2 - \theta_4^2, \quad \theta_4^2 > 0, \quad \mu_4^2 > 0. \quad (32d)$$

Note that Eq. (31) is one set of solutions for Eq. (30). The boundary conditions of plate at  $X_1 = 0$  and  $X_1 = 1$  are assumed simply supported, then Eq. (31) are reduced as follow:

$$W_1 = [A_1 \sinh(\mu_1 X_2) + A_2 \cosh(\mu_1 X_2)] \sin(\theta_1 X_1), \quad (33a)$$

$$W_2 = [A_5 \sinh(\mu_2 X_2) + A_6 \cosh(\mu_2 X_2)] \sin(\theta_2 X_1), \quad (33b)$$

$$W_2 = [A_5 \sinh(\mu_2 X_2) + A_6 \cosh(\mu_2 X_2)] \sin(\theta_2 X_1), \quad (33b)$$

$$W_3 = [A_9 \sin(\mu_3 X_2) + A_{10} \cos(\mu_3 X_2)] \sin(\theta_3 X_1) \quad (33c)$$

$$W_4 = [A_{13} \sinh(\mu_4 X_2) + A_{14} \cosh(\mu_4 X_2)] \cos(\theta_4 X_1) \quad (33d)$$

and

$$\theta_1 = \theta_2 = \theta_3 = \theta_4 = m\pi. \quad (34)$$

Substituting Eqs. (33) into Eqs. (29) and substituting the results into the three appropriate boundary conditions along the edges at  $X_2 = 0$  and  $X_2 = 1$  (Eqs. (11)), leads to a characteristic determinant of the eight-order for each  $m$ . Expanding the determinant and collecting terms yield a characteristic equation.

### 3. Comparison Studies

In order to validate the accuracy of the present method, a comparison has been carried out with the previously published results by Leissa [25], Liew et al. [26], Hosseini-Hashemi and Arsanjani [16], Malik and Bert [28], and Zhou et al. [30] for both thin ( $\tau=0.001$ ) and moderately thick ( $\tau=0.1$  and  $\tau=0.2$ ) isotropic square plates for all the six considered boundary conditions. The present results are shown in Tables 1 and 2, and are compared with other well-known solutions (e.g. exact solution by Hosseini-Hashemi and Arsanjani [16], Rayleigh Ritz method by Leissa [25], Liew et al. [26] and Zhou et al. [30] and differential quadrature method by Malik and Bert [28]) and different plate theories (e.g. classical plate theory by Leissa [25], first-order shear deformation plate theory by Hosseini-Hashemi and Arsanjani [16]) and three dimensional elasticity (by Leissa et al. [25], Liew et al. [26], and Zhou et al. [30]). From the results shown in Table 1, it can be observed that there is an excellent agreement between the present results and those given by Leissa [25], Liew et al. [26], Hosseini-Hashemi and Arsanjani [16], Malik and Bert [28], and Zhou et al. [30].

### 4. Results and Discussion

The natural frequency parameters obtained from the exact characteristic equations presented in Section 3 have been expressed in dimensionless form  $\beta$  where the symbols are defined in Section 2. The numerical calculations have been performed for each of the six different boundary conditions. In the numerical calculations, Poisson's ratio  $\nu=0.3$  has been used. The results are given in Table 2 for the thickness to length ratios  $\tau=0.001$ ,  $\tau=0.1$ , and  $\tau=0.2$  over a range of aspect ratios  $\eta = 0.5$  and  $\eta = 2$ . In Table 2, the results are given for the first five non-dimensional natural frequency parameters of the isotropic rectangular plates. The results are pre-

sented with considerable accuracy simply because they are easily obtained for the accuracy given, and because they may be used as a benchmark. For all six cases the wave forms are, of course, sine functions in the  $x_1$  direction, according to their corresponding equations of transverse displacement. Furthermore, the wave forms in the  $x_2$  direction are sine function exactly for the  $S_h S_h S_h S_h$  case only, whereas for the other cases the forms are only approximately sinusoidal.

#### 4.1. The effect of plate aspect ratio on the natural frequency parameters

In order to study the effect of aspect ratio on the vibration behavior of the plates, consideration may now be focused on Tables 2-4 and Figure 2. From the results presented in these tables, it is observed that the nondimensional natural frequency parameter  $\beta$ , except for the first nondimensional natural frequency of the  $S_h F S_h F$  plates, for the rest of considered six plates increases with increasing plate aspect ratio ( $a/b$ ), if the relative thickness ratio  $\tau$  is kept constant. It seems this different behavior of  $S_h F S_h F$  plates, with respect to the rest of plates, is due to having two parallel edges free boundary conditions. Considering the results presented in Table 3 and Figure 2, one may observe that, the half wave in the  $x_1$  direction decreases and the half waves in the  $x_2$  direction increase with increasing plate aspect ratio ( $a/b$ ), if the relative thickness ratio  $\tau$  is kept constant. This observation indicates that, between two plates having an identical  $b$ , thickness  $h$  and boundary conditions, the one which has longer width  $a$  behaves like a beam.

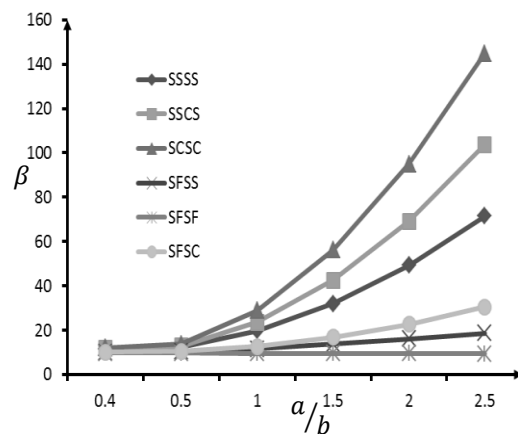


Figure 2. The effects of aspect ratio on the nondimensional frequency ( $\tau = 0.1$ ).

**Table 1.** The comparison study of the natural frequency parameter ( $\beta = a\omega^2 \sqrt{\rho h / D}$ ) for  $S_h S_h S_h S_h$ ,  $S_h S_h S_h C$ ,  $S_h C S_h C$ ,  $S_h F S_h F$ ,  $S_h S_h S_h F$  and  $S_h C S_h F$  boundary conditions of square plate for different thickness ratios.

BCs	Methods	$\tau = \frac{h}{a}$	$\beta_1$	$\beta_2$	$\beta_3$	$\beta_4$	$\beta_5$
$S_h S_h S_h S_h$	Malik [28]	0.1	19.0901	45.6193	45.6193	70.1040	85.4878
	Liew et al [26]		19.0898	45.6193	45.6193	70.1038	85.4876
	Zhou et al [30]		19.0898	45.6193	45.6193	70.1038	85.4876
	Present study		19.0661	45.4917	45.4917	69.8213	85.0830
$S_h S_h S_h C$	Hashemi [16]	0.1	22.4260	47.2245	52.3247	74.4019	86.2191
	Malik [28]		22.4535	47.2761	52.4356	74.5481	86.3542
	Present study		22.4047	47.1387	52.2487	74.2516	85.9542
$S_h C S_h C$	Hashemi [16]	0.2	22.5355	40.0654	45.3350	59.3313	66.0079
	Present study		22.5597	40.1049	45.4333	59.4424	66.1755
$S_h F S_h F$	Leissa [25]	0.001	9.6314	16.1348	36.7256	38.9450	46.7381
	Hashemi [16]		9.6311	16.1313	36.7161	38.9433	46.7317
	Present study		9.6310	16.1314	36.7165	38.9436	46.7319
$S_h S_h S_h F$	Hashemi [16]	0.2	10.6981	23.1532	32.7157	43.5740	45.3051
	Malik [28]		10.7216	23.2565	32.9299	43.9289	45.6888
	Present study		10.8240	23.5908	31.8004	44.5052	45.8714
$S_h C S_h F$	Hashemi [16]	0.1	12.2606	30.4743	38.7128	55.9736	62.9527
	Malik [28]		12.2623	30.5095	38.7264	56.0240	63.0725
	Present study		12.2519	30.4373	38.6425	55.8560	62.8485

**Table 2.** The first five natural frequency parameters ( $\beta = a\omega^2 \sqrt{\rho h / D}$ ) for  $S_h S_h S_h S_h$ ,  $S_h S_h S_h C$ ,  $S_h C S_h C$ ,  $S_h F S_h F$ ,  $S_h S_h S_h F$  and  $S_h C S_h F$  boundary conditions of rectangular plates with different aspect and thickness ratios.

BCs	$\tau = \frac{h}{a}$	$\eta = \frac{b}{a}$	$\beta_1$	$\beta_2$	$\beta_3$	$\beta_4$	$\beta_5$
$S_h S_h S_h S_h$	0.001	0.5	49.3476	78.9557	128.302	167.778	197.385
	0.1		45.4917	69.8213	106.765	133.770	152.821
	0.2		38.2052	55.2943	95.4108	106.562	106.562
	0.001	2	12.3370	19.7391	32.0760	41.9455	49.3476
	0.1		12.0678	19.0661	30.3643	45.4917	45.4917
	0.2		11.3729	17.4553	26.6913	33.4425	38.2052
$S_h S_h S_h C$	0.001	0.5	69.3257	94.5830	140.200	206.688	208.381
	0.1		59.4495	79.1242	112.462	151.451	156.336
	0.2		45.4333	59.4424	81.3549	101.807	107.923
	0.001	2	12.9185	21.5335	35.2111	42.2393	50.4307
	0.1		12.5941	20.6199	32.8994	39.3201	46.2699
	0.2		11.7847	18.5629	28.2848	33.5677	38.6280
$S_h C S_h C$	0.001	0.5	95.2594	115.799	156.350	218.961	254.120
	0.1		75.3708	90.2390	119.256	160.420	168.269
	0.2		53.3295	64.1280	83.9169	107.449	109.436
	0.001	2	13.6857	23.6462	38.6936	42.5863	51.6737
	0.1		13.2755	22.4047	35.6292	39.5722	47.1387
	0.2		12.2972	19.7810	29.9276	33.7067	39.0840
$S_h F S_h F$	0.001	0.5	9.5076	27.3596	38.4758	64.2026	87.0925
	0.1		9.3259	24.9369	35.9366	56.4028	75.9733
	0.2		8.8851	21.2688	30.9574	45.1618	59.2599
	0.001	2	9.7322	11.6743	17.6556	27.7016	39.1518
	0.1		9.5554	11.3716	16.8869	26.1218	36.5820
	0.2		9.0899	10.7008	15.5425	23.1668	31.5120
$S_h S_h S_h F$	0.001	0.5	16.1141	46.6708	75.1191	95.83-3	110.659
	0.1		15.5981	43.2958	66.8379	83.4127	94.3631
	0.2		14.5425	37.0571	53.4665	65.3572	72.7286
	0.001	2	10.2961	14.7587	23.6025	37.0899	39.4497
	0.1		10.1062	14.3659	22.6312	34.8247	36.9407
	0.2		9.23518	13.4236	20.4762	30.2362	31.8004
$S_h C S_h F$	0.001	0.5	22.8153	50.7489	98.7753	99.7726	132.256
	0.1		21.1679	45.4951	81.0143	83.8251	103.514
	0.2		18.4830	37.4621	58.4731	64.0231	73.6141
	0.001	2	10.4221	15.7439	25.7668	40.5452	40.5831
	0.1		10.1999	15.1839	24.3551	37.1590	37.4081
	0.2		9.66068	13.9690	21.5178	31.6148	31.9010

**Table 3.** The first six natural frequency parameters ( $\beta = a\omega^2 \sqrt{\rho h / D}$ ) in terms of wave numbers (m,n) with different aspect and thickness ratios 0.1.

BCs	$\eta = \frac{b}{a}$	$\beta_1$	$\beta_2$	$\beta_3$	$\beta_4$	$\beta_5$	$\beta_6$
$S_h S_h S_h S_h$	1	19.0661 <sup>11</sup>	45.4917 <sup>12</sup>	45.4917 <sup>21</sup>	69.8213 <sup>22</sup>	85.0830 <sup>13</sup>	85.0830 <sup>31</sup>
	2	12.0678 <sup>11</sup>	19.0661 <sup>12</sup>	30.3643 <sup>13</sup>	39.1012 <sup>21</sup>	45.4917 <sup>14</sup>	45.4917 <sup>22</sup>
	4	10.2908 <sup>11</sup>	12.0678 <sup>12</sup>	15.0048 <sup>13</sup>	19.0661 <sup>14</sup>	24.2047 <sup>15</sup>	30.3643 <sup>16</sup>
$S_h S_h S_h C$	1	22.4047 <sup>11</sup>	47.1387 <sup>21</sup>	52.2487 <sup>12</sup>	74.2516 <sup>22</sup>	85.9542 <sup>31</sup>	93.5508 <sup>13</sup>
	2	12.5941 <sup>11</sup>	20.6199 <sup>12</sup>	32.8994 <sup>13</sup>	39.3201 <sup>21</sup>	46.2699 <sup>22</sup>	48.8053 <sup>14</sup>
	4	10.3583 <sup>11</sup>	12.314 <sup>12</sup>	15.4919 <sup>13</sup>	19.8146 <sup>14</sup>	25.2095 <sup>15</sup>	31.6067 <sup>16</sup>
$S_h C S_h C$	1	26.7154 <sup>11</sup>	49.1887 <sup>21</sup>	59.4495 <sup>12</sup>	79.1242 <sup>22</sup>	86.9675 <sup>31</sup>	102.059 <sup>13</sup>
	2	13.2755 <sup>11</sup>	22.4047 <sup>12</sup>	35.6292 <sup>13</sup>	39.5722 <sup>21</sup>	47.1387 <sup>22</sup>	52.2487 <sup>14</sup>
	4	10.4375 <sup>11</sup>	12.5941 <sup>12</sup>	16.0293 <sup>13</sup>	20.6199 <sup>14</sup>	26.2699 <sup>15</sup>	32.8994 <sup>16</sup>
$S_h S_h S_h F$	1	11.3742 <sup>11</sup>	26.1599 <sup>12</sup>	38.2947 <sup>21</sup>	53.2655 <sup>22</sup>	55.6363 <sup>13</sup>	78.4086 <sup>31</sup>
	2	10.0877 <sup>11</sup>	14.3168 <sup>12</sup>	22.5325 <sup>13</sup>	34.6888 <sup>14</sup>	36.9407 <sup>21</sup>	41.2450 <sup>22</sup>
	4	9.75542 <sup>11</sup>	10.8963 <sup>12</sup>	13.1282 <sup>13</sup>	16.4284 <sup>14</sup>	20.7768 <sup>15</sup>	26.1507 <sup>16</sup>
$S_h F S_h F$	1	9.4411 <sup>11</sup>	15.3930 <sup>12</sup>	33.8671 <sup>13</sup>	36.3482 <sup>21</sup>	42.8076 <sup>22</sup>	62.1701 <sup>23</sup>
	2	9.5550 <sup>11</sup>	11.3742 <sup>12</sup>	16.8862 <sup>13</sup>	26.1599 <sup>14</sup>	36.5816 <sup>21</sup>	38.2947 <sup>22</sup>
	4	9.6014 <sup>11</sup>	10.0877 <sup>12</sup>	12.5672 <sup>13</sup>	14.3168 <sup>14</sup>	20.5112 <sup>15</sup>	22.5325 <sup>16</sup>
$S_h C S_h F$	1	12.3683 <sup>11</sup>	30.9013 <sup>12</sup>	38.8830 <sup>21</sup>	56.5808 <sup>22</sup>	63.4517 <sup>13</sup>	79.0018 <sup>31</sup>
	2	10.2307 <sup>11</sup>	15.2821 <sup>12</sup>	24.5504 <sup>13</sup>	37.2648 <sup>21</sup>	37.6711 <sup>14</sup>	41.8102 <sup>22</sup>
	4	9.6959 <sup>11</sup>	11.0474 <sup>12</sup>	13.4962 <sup>13</sup>	17.0589 <sup>14</sup>	21.6826 <sup>15</sup>	36.9409 <sup>16</sup>

<sup>mn</sup>; m is the mode sequence in x direction and n is

**4.2. The effect of plate thickness ratio ( $\tau = h/a$ ) on the natural frequency parameters**

The influence of thickness ratio  $\tau$  on the nondimensional natural frequency parameter  $\beta$  can also be examined for plates with specific boundary conditions by keeping the aspect ratio constant while varying the thickness ratio. From the results presented in Tables 1-3 and Figure 3, it can be easily observed that, as the thickness ratio  $\tau$  increases from 0.001 to 0.2 the nondimensional natural frequency parameter decreases. Such behavior is due to the influence of the transverse shear deformation in the plates.

**4.3. The effect of plate boundary conditions on the natural frequency parameters**

To study the effect of boundary conditions on the nondimensional natural frequency parameter  $\beta$ , consideration may now be focused on the values of  $\beta$  listed in a specific column of Tables 1-3. From the results presented in these tables, it is observed that the lowest nondimensional natural frequency parameter corresponds to plates subjected to less edge constraints. As the number of supported edges increases, the values of  $\beta$  also increase. Among all six

boundary conditions listed in Tables 1-3, it can be seen that the lowest and highest values of  $\beta$  correspond to  $S_h F S_h F$  and  $S_h C S_h C$  cases, respectively. Thus, the higher constraints at the edges increase the flexural rigidity of the plate, resulting in a higher nondimensional natural frequency parameter response.

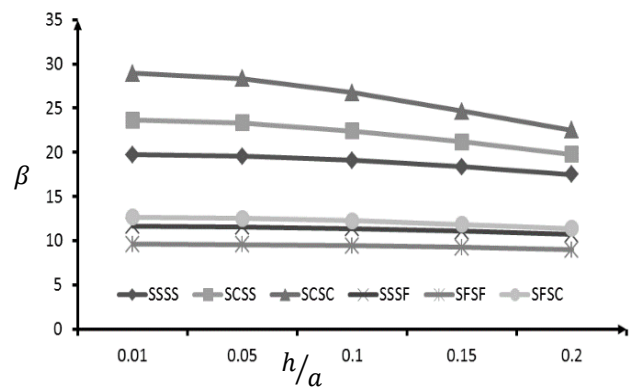


**Figure 3.** The effects of thickness to length ratio on the nondimensional frequency ( $\eta = 1$ ).

#### 4.4. Complementary results

In order to satisfy Eq. (35) (case of  $S_h S_h S_h S_h$  boundary conditions), it is necessary that

$$\sinh[\eta\mu_1]\sinh[\eta\mu_2]\sin[\eta\mu_3]\sinh[\eta\mu_4] = 0 \quad (35)$$

$$\sin(\eta\mu_3) = 0, \quad \mu_3 = \frac{n\pi}{\eta} \quad (36)$$

Where  $n$  ( $n = 1, 2, 3, \dots$ ) is integer values.

Using Eq. (36), between two plates having identical thickness ratio and boundary condition, the dimensionless natural frequency  $\beta$  given in Table 3 for  $n$ ,  $m$  and  $\eta$ , may be related to  $\dot{n}$ ,  $\dot{m}$  and  $\dot{\eta}$  through Eq. (37).

$$\left(\frac{n\pi}{\eta}\right)^2 + (m\pi)^2 = \left(\frac{\dot{n}\pi}{\dot{\eta}}\right)^2 + (\dot{m}\pi)^2 \quad (37)$$

As an example for two simply supported plates having identical thickness ratio and mode number in  $x_1$  direction ( $\dot{m} = m$ ), the nondimensional natural frequency parameter for  $\eta = 1$  and  $n = 1$  ( $\beta = 19.7391$ ) is the same as those of  $\dot{\eta} = 2$  and  $\dot{n} = 2$ , because

$$\left(\frac{n\pi}{\eta}\right)^2 = \left(\frac{\dot{n}\pi}{\dot{\eta}}\right)^2 \rightarrow n\dot{\eta} = \dot{n}\eta = (1)(2) = (2)(1) \quad (38)$$

This is because for  $\dot{n} = 2$ , the simply supported boundary condition of selected plate is duplicated at the nodal lines ( $x_2 = b/2$ ). Similarly, for two simply supported plates having identical thickness ratio and mode number in  $x_2$  direction ( $\dot{n} = n$ ), the nondimensional natural frequency parameter for  $\eta = 1$  and  $m = 2$  ( $\beta = 49.3476$ ) is the same as those of  $\dot{\eta} = 1/2$  and  $\dot{m} = 1$ ,

$$\left(\frac{1}{\eta}\right)^2 + (m)^2 = \left(\frac{1}{\dot{\eta}}\right)^2 + (\dot{m})^2 = \left(\frac{1}{1}\right)^2 + (2)^2 = (2)^2 + (1)^2. \quad (39)$$

Focusing now on two simply supported plates having identical thickness ratio, the nondimensional natural frequency parameter for  $\eta = 1$ ,  $m = 1$  and  $n = 1$  ( $\beta = 10.0661$ ) is the same as those of  $\dot{\eta} = 4$ ,  $\dot{m} = 1$  and  $\dot{n} = 4$ . Thus, some additional results regarding other mode numbers in  $x_1$  and  $x_2$  directions and aspect ratio not covered in Tables 1 and 3, can be obtained from the same table through Eq. (93).

## 5. Conclusions

In this study the trigonometric shear deformation plate theory is used to study the flexural vibration behavior of moderately thick rectangular with different boundary conditions. The exact closed-form vibration equations are derived from the six cases having two opposite edges simply supported hard and any of the other two edges can be hard simply supported, clamped or free. The six cases considered are namely:  $S_h S_h S_h S_h$ ,  $S_h S_h S_h C$ ,  $S_h C S_h C$ ,  $S_h F S_h F$ ,  $S_h S_h S_h F$  and  $S_h C S_h F$  plates. The ad-

vantages of the proposed closed-form solution are the following:

1- They are capable of predicting the natural frequency parameters with high accuracy within the validity of the trigonometric shear deformation plate theory since an exact analytical solution is used.

2- They provide a closed-form vibration equation that can be easily solved numerically by researchers and engineers.

Using numerical data provided previously, the effect of different parameters including boundary conditions, aspect ratio and thickness ratio on the nondimensional natural frequency parameter is examined and discussed in detail. The obtained results show the accuracy of the trigonometric shear deformation plate theory. The nondimensional natural frequency parameter  $\beta$ , except for the first nondimensional natural frequency of the  $S_h F S_h F$  plates, decreases with increasing plate aspect ratio. The nondimensional natural frequency parameter of the plate increases monotonically, as the thickness ratio increases. For all values of aspect ratio and thickness ratio, the nondimensional natural frequency parameter corresponding to clamped boundary conditions possesses higher values in comparison with free and simply supported boundary conditions.

## Appendix A

In this section, the Hamilton's principle is used to obtain the governing differential equation for free vibration of moderately thick isotropic rectangular plates under the hypothesis of the trigonometric shear deformation theory. The Hamilton's principle is obtained as follows:

$$\int_0^t \delta(U - T) dt = 0, \quad (A1)$$

Where  $T$  is the kinetic energy of the plate and  $U$  is the elastic strain energy of the plate. The kinetic energy, including rotary inertia, and the elastic strain energy are given by the following equation:

$$\delta T = \rho \int_{-h/2}^{h/2} \int_0^b \int_0^a \left( \frac{\partial^2 u}{\partial t^2} \delta u + \frac{\partial^2 v}{\partial t^2} \delta v + \frac{\partial^2 w}{\partial t^2} \delta w \right) dx_1 dx_2 dx_3, \quad (A2)$$

$$\delta U = \int_{-h/2}^{h/2} \int_0^b \int_0^a (\sigma_1 \delta \varepsilon_1 + \sigma_2 \delta \varepsilon_2 + \tau_{23} \delta \gamma_{23} + \tau_{13} \delta \gamma_{13} + \tau_{12} \delta \gamma_{12}) dx_1 dx_2 dx_3. \quad (A3)$$

According to the trigonometric shear deformation theory, the following strain-displacement relations are given:

$$\varepsilon_1 = -x_3 \frac{\partial^2 w}{\partial x_1^2} + f(x_3) \frac{\partial \varphi_1}{\partial x_1}, \tag{A4}$$

$$\varepsilon_2 = -x_3 \frac{\partial^2 w}{\partial x_2^2} + f(x_3) \frac{\partial \varphi_2}{\partial x_2}, \tag{A5}$$

$$\gamma_{13} = \frac{\partial f(x_3)}{\partial x_3} \varphi_1, \tag{A6}$$

$$\gamma_{23} = \frac{\partial f(x_3)}{\partial x_3} \varphi_2, \tag{A7}$$

$$\gamma_{21} = -2x_3 \frac{\partial^2 w}{\partial x_1 \partial x_2} + f(x_3) \left( \frac{\partial \varphi_1}{\partial x_2} + \frac{\partial \varphi_2}{\partial x_1} \right). \tag{A8}$$

Substituting Eqs. (A4-A8) into Eqs. (A2-A3), the Eq. (A1) can be rewritten as what follows:

$$\int_0^t \left\{ \int_0^a \int_0^b \left[ \left( \frac{\partial^2 M_1}{\partial x_1^2} + 2 \frac{\partial^2 M_{12}}{\partial x_1 \partial x_2} + \frac{\partial^2 M_2}{\partial x_2^2} - I_1 \frac{\partial^2 w}{\partial t^2} \right. \right. \right. \\ \left. \left. - I_2 \left( \frac{\partial^4 w}{\partial t^2 \partial x_1^2} + \frac{\partial^4 w}{\partial t^2 \partial x_2^2} \right) \right. \right. \\ \left. \left. - I_3 \left( \frac{\partial^3 \varphi_1}{\partial x_1 \partial t^2} + \frac{\partial^3 \varphi_2}{\partial x_2 \partial t^2} \right) \right] \delta w \right. \\ \left. + \left( \frac{\partial N_{s1}}{\partial x_1} + \frac{\partial N_{s21}}{\partial x_2} - N_{Tc1} \right. \right. \\ \left. \left. + I_3 \frac{\partial^3 w}{\partial t^2 \partial x_1} - I_4 \frac{\partial^2 \varphi_1}{\partial t^2} \right) \delta \varphi_1 \right. \\ \left. + \left( \frac{\partial N_{s2}}{\partial x_2} + \frac{\partial N_{s21}}{\partial x_1} - N_{Tc2} \right. \right. \\ \left. \left. - I_3 \frac{\partial^3 w}{\partial t^2 \partial x_2} \right. \right. \\ \left. \left. + I_4 \frac{\partial^2 \varphi_2}{\partial t^2} \right) \delta \varphi_2 \right\} dx_1 dx_2 dt \\ = 0, \tag{A9}$$

Where the stress resultants ( $M_{ij}$ ,  $M_i$ ,  $N_{sij}$ ,  $N_{si}$  and  $N_{Tci}$ ) are defined by:

$$(M_1, M_2, M_{12}) = \int_{-\frac{h}{2}}^{\frac{h}{2}} (\sigma_1, \sigma_2, \tau_{12}) dx_3, \tag{A10}$$

$$(N_{s1}, N_{s2}, N_{s12}) \tag{A11}$$

$$= \int_{-\frac{h}{2}}^{\frac{h}{2}} (\sigma_1, \sigma_2, \tau_{12}) f(x_3) dx_3, \tag{A12}$$

$$(N_{Tc1}, N_{Tc2}) = \int_{-\frac{h}{2}}^{\frac{h}{2}} (\tau_{31}, \tau_{32}) \frac{\partial f(x_3)}{\partial x_3} dx_3, \tag{A12}$$

According to the trigonometric shear deformation theory, the following stress-displacement relations, under the hypothesis  $\sigma_3 = 0$ , are given:

$$\sigma_1 = \frac{E}{1 - \nu^2} \left( -x_3 \left( \frac{\partial^2 w}{\partial x_1^2} + \nu \frac{\partial^2 w}{\partial x_2^2} \right) \right. \\ \left. + f(x_3) \left( \frac{\partial \varphi_1}{\partial x_1} + \nu \frac{\partial \varphi_2}{\partial x_2} \right) \right), \tag{A13}$$

$$\sigma_2 = \frac{E}{1 - \nu^2} \left( -x_3 \left( \frac{\partial^2 w}{\partial x_2^2} + \nu \frac{\partial^2 w}{\partial x_1^2} \right) \right. \\ \left. + f(x_3) \left( \frac{\partial \varphi_2}{\partial x_2} + \nu \frac{\partial \varphi_1}{\partial x_1} \right) \right), \tag{A14}$$

$$\tau_{12} = \frac{E}{2(1 + \nu)} \left( -2x_3 \frac{\partial^2 w}{\partial x_1 \partial x_2} \right. \\ \left. + f(x_3) \left( \frac{\partial \varphi_2}{\partial x_1} + \frac{\partial \varphi_1}{\partial x_2} \right) \right), \tag{A15}$$

$$\tau_{13} = \frac{E}{2(1 + \nu)} \frac{\partial f(x_3)}{\partial x_3} \varphi_1, \tag{A16}$$

$$\tau_{32} = \frac{E}{2(1 + \nu)} \frac{\partial f(x_3)}{\partial x_3} \varphi_2, \tag{A17}$$

Finally, the governing differential equations of motion are given in absence of the applied load and in terms of the stress resultants by Hamilton's principle as follows:

$$\delta w: \left( \frac{\partial^2 M_1}{\partial x_1^2} + 2 \frac{\partial^2 M_{12}}{\partial x_1 \partial x_2} + \frac{\partial^2 M_2}{\partial x_2^2} - I_1 \frac{\partial^2 w}{\partial t^2} \right. \\ \left. - I_2 \left( \frac{\partial^4 w}{\partial t^2 \partial x_1^2} + \frac{\partial^4 w}{\partial t^2 \partial x_2^2} \right) \right. \\ \left. - I_3 \left( \frac{\partial^3 \varphi_1}{\partial x_1 \partial t^2} + \frac{\partial^3 \varphi_2}{\partial x_2 \partial t^2} \right) \right) \\ = 0, \tag{A18}$$

$$\delta \varphi_1: \left( \frac{\partial N_{s1}}{\partial x_1} + \frac{\partial N_{s21}}{\partial x_2} - N_{Tc1} + I_3 \frac{\partial^3 w}{\partial t^2 \partial x_1} \right. \\ \left. - I_4 \frac{\partial^2 \varphi_1}{\partial t^2} \right) = 0, \tag{A19}$$

$$\delta \varphi_2: \left( \frac{\partial N_{s2}}{\partial x_2} + \frac{\partial N_{s21}}{\partial x_1} - N_{Tc2} \right. \\ \left. - I_3 \frac{\partial^3 w}{\partial t^2 \partial x_2} + I_4 \frac{\partial^2 \varphi_2}{\partial t^2} \right) \\ = 0. \tag{A20}$$

## References

- [1] Leissa AW, Recent Studies in Plate Vibration 1982-1985, Part-I Classical Theory, *Shock Vib Digest*, 1987; 19(3): 11-18.
- [2] Reissner E, On the theory of bending of elastic plates. *J Math Phys*, 1944; 23(3): 184-191.
- [3] Reissner E, The effect of transverse shear deformation on the bending of elastic plates. *ASME J Appl Mech*, 1945; 12(5): 69-77.
- [4] Mindlin RD, Influence of rotatory inertia and shear on flexural motions of isotropic, elastic plates. *ASME J Appl Mech*, 1951; 18(5): 31-38.

- [5] Kim J, Cho M, Enhanced first-order shear deformation theory for laminated and sandwich plates. *J Appl Mech*, 2005; 72(6): 809–817.
- [6] Reddy JN, **Theory and analysis of elastic plates and shells**. CRC Press, 2007.
- [7] Ferreira AJM, Roque CMC, Jorge RMN, Electrochemical Analysis of composite plates by trigonometric shear deformation theory and multi quadrics. *Comput Struct*, 2005; 83(1): 2225–2237.
- [8] Xiang S, Wang KM, Free vibration analysis of symmetric laminated composite plates by trigonometric shear deformation theory and inverse multi quadric RBF. *Thin-Walled Struct*, 2009; 47(6): 304–310.
- [9] Mantari JL, Oktem AS, Guedes Soares C, A new trigonometric shear deformation theory for isotropic, laminated composite and sandwich plates. *Int J Solids Struct*, 2012; 49(4): 43–53.
- [10] Mantari JL, Oktem AS, Guedes Soares C, A new trigonometric layerwise shear deformation theory for the finite element analysis of laminated composite and sandwich plates. *Comput Struct*, 2012; 94(7): 45–53.
- [11] Tounsi A, Houari MSA, Benyoucef S, Bedia EAA, A refined trigonometric shear deformation theory for thermoelastic bending of functionally graded sandwich plates. *Aero Sci Technol*, 2013; 24(6): 209–220.
- [12] Tornabene F, Viola E, Fantuzzi N, General higher-order equivalent single layer theory for free vibrations of doubly-curved laminated composite shells and panels. *Compos Struct*, 2013; 104(31): 94–117.
- [13] Rango RF, Nallim LG, Oller S, Formulation of enriched macro elements using trigonometric shear deformation theory for free vibration analysis of symmetric laminated composite plate assemblies. *Compos Struct*, 2015; 119(2): 38–49.
- [14] Sahoo R, Singh BN, A new trigonometric zigzag theory for static analysis of laminated composite and sandwich plates. *Aero Sci Technol*, 2014; 35(5): 15–28.
- [15] Vel SS, Batra RC, Three-dimensional exact solution for the vibration of functionally graded rectangular plates. *J Sound Vib*, 2004; 272: 703–730.
- [16] Hosseini-Hashemi S, Arsanjani M, Exact characteristic equations for some of classical boundary conditions of vibrating moderately thick rectangular plates. *Int J Solids Struct*, 2005; 42(10): 819–853.
- [17] Hosseini-Hashemi S, Khorshidi K, Amabili, M, Exact solution for linear buckling of rectangular Mindlin plates. *J Sound Vib*, 2008; 315(3): 318–342.
- [18] Hosseini-Hashemi S, Khorshidi K, Rokni Damavandi Taher H, Exact acoustical analysis of vibrating rectangular plates with two opposite edges simply supported via Mindlin plate theory. *J Sound Vib*, 2009; 322(3): 883–900.
- [19] Hosseini-Hashemi S, Rokni Damavandi Taher H, Akhavan H, Omidi M, Free vibration of functionally graded rectangular plates using first-order shear deformation plate theory. *Int J Eng Sci*, 2010; 34(2): 1276–1291.
- [20] Khorshidi K, Elasto-plastic response of impacted moderately thick rectangular plates with different boundary conditions. *Procedia Eng*, 2011; 10(2): 1742–1747.
- [21] Khorshidi K, Vibro-acoustic analysis of Mindlin rectangular plates resting on an elastic foundation. *Sci Iranica*, 2008; 18(1): 45–52.
- [22] Hosseini-Hashemi S, Fadaee M, Atashipour SR, A new exact analytical approach for free vibration of Reissner–Mindlin Functionally graded rectangular plates. *Int J Mech Sci*, 2011; 53(7): 11–22.
- [23] Liu, B., Xing, Y., Exact solutions for free vibrations of orthotropic rectangular Mindlin plates. *Compos Struct*, 2011. 93(4): 1664–1672.
- [24] Dozio L, Exact vibration solutions for cross-ply laminated plates with two opposite edges simply supported using refined theories of variable order. *J Sound Vib*, 2014; 333(2): 2347–2359.
- [25] Leissa AW, The free vibration of rectangular plates. *J Sound Vib*, 1973; 31(3): 257–293.
- [26] Liew KM, Xiang Y, Kitipornchai S, Transverse vibration of thick rectangular plates-I. Comprehensive sets of boundary conditions. *Comput Struct*, 1993; 49(1): 1–29.
- [27] Liew KM, Hung KC, Lim MK, Vibration of Mindlin plates using boundary characteristic orthogonal polynomials. *J Sound Vib*, 1995; 182(1): 77–90.

- [28] Malik M, Bert CW, Three-dimensional elasticity solutions for free vibrations of rectangular plates by the differential quadrature method. *Int J Solids Struct*, 1998; 35(4): 299–318.
- [29] Liew KM, Hung KC, Lim MK, A continuum three-dimensional vibration analysis of thick rectangular plates. *Int J Solids Struct*, 1993; 30(24): 3357–3379.
- [30] Zhou D, Cheung YK, Au FTK, Lo SH, Three-dimensional vibration analysis of thick rectangular plates using Chebyshev polynomial and Ritz method. *Int J Solids Struct*, 2002; 196(49): 4901–4910.